Beware of Your Cre-Ation: *lacZ* Expression Impairs Neuronal Integrity and Hippocampus-Dependent Memory

J.M. Reichel,[1,2] B.T. Bedenk,[1,3] N.C. Gassen,[4] K. Hafner,[4] S.A. Bura,[1] S. Almeida-Correa,[1] A. Genewsky,[1] N. Dedic,[1] F. Giesert,[5] A. Agarwal,[6] K.-A. Nave,[7] T. Rein,[4] M. Czisch,[1,3] J.M. Deussing,[1] and C.T. Wotjak[1]*

ABSTRACT: Expression of the *lacZ*-sequence is a widely used reporter-tool to assess the transgenic and/or transfection efficacy of a target gene in mice. Once activated, *lacZ* is permanently expressed. However, protein accumulation is one of the hallmarks of neurodegenerative diseases. Furthermore, the protein product of the bacterial *lacZ* gene is ß-galactosidase, an analog to the mammalian senescence-associated ß-galactosidase, a molecular marker for aging. Therefore we studied the behavioral, structural and molecular consequences of *lacZ* expression in distinct neuronal sub-populations. *lacZ* expression in cortical glutamatergic neurons resulted in severe impairments in hippocampus-dependent memory accompanied by marked structural alterations throughout the CNS. In contrast, GFP expression or the expression of the ChR2/YFP fusion product in the same cell populations did not result in either cognitive or structural deficits. GABAergic *lacZ* expression caused significantly decreased hyper-arousal and mild cognitive deficits. Attenuated structural and behavioral consequences of *lacZ* expression could also be induced in adulthood, and *lacZ* transfection in neuronal cell cultures significantly decreased their viability. Our findings provide a strong caveat against the use of *lacZ* reporter mice for phenotyping studies and point to a particular sensitivity of the hippocampus formation to detrimental consequences of *lacZ* expression. © 2016 Wiley Periodicals, Inc.

KEY WORDS: hippocampus; volume loss; neurodegeneration; neurotoxicity; transgenic; cognition; memory impairment

INTRODUCTION

The bacterial *lacZ* gene codes for *ß*-galactosidase (β-gal) which can be easily visualized by histochemical staining (Sanes et al., 1986; Bonnerot et al., 1987; Cui et al., 1994; Schmidt et al., 1998; Soriano, 1999). Mechanistically, *lacZ* expression is mediated by the Cre/*loxP* system (Hoess et al., 1982; Branda and Dymecki, 2004), and once Cre-recombination has occurred, *lacZ* is continuously expressed. Transgenic (co-)expression of *lacZ* is a widely used reporter to assess the temporal and spatial expression of genes of interest in vitro and in vivo in mice (Price et al., 1987; Nolan et al., 1988; Soriano, 1999; Skarnes et al., 2011). Hundreds of conventional transgenic mouse lines listed by the Jackson laboratory (http://www.jax.org/index.html) also contain the Rosa26-*lacZ* locus (http://jaxmice.jax.org/list/ra1510.html; http://jaxmice.jax.org/list/xprs_laczRT.html), but this fact is rarely acknowledged in current studies. Moreover, recent studies have in fact advertised the generation of transgenic mouse repositories in order to target every protein coding gene and visualize the genetic manipulation via *lacZ* expression (Skarnes et al., 2011; White et al., 2013). Recent initiatives (e.g. EMPReSS (de Angelis et al., 2015)) are aimed at phenotyping 20.000 different mouse mutants, with most of them expressing *lacZ* (https://www.mousephenotype.org/impress). Additionally, there are a number of methodological techniques that require the co-expression of *lacZ*. For instance the Daun02 inactivation method (Koya et al., 2009; Cruz et al., 2015). This method employs the *Fos*-coupled *lacZ*-expression in a cell population of interest, and the expressing cells can subsequently be selectively silenced via the prodrug Daun02 [reviewed in (Cruz et al., 2013)]. This method is widely used in addiction research as well as learning and memory research and has been applied in mice, rats and monkeys (Cruz et al., 2013; Cruz et al., 2014; Engeln et al., 2016).

There are various theoretical aspects arguing against the use of *lacZ* expression in transgenic mice. For instance, β-gal may accumulate in the affected cells due to the continuous expression of *lacZ*. Continuous protein accumulation, however, represents one of the hallmarks of neurodegenerative diseases, which are associated with severe cognitive and structural deficits (Braak and Braak, 1991, 2000; Kobayashi and Chen, 2005; Abdul et al., 2009). Moreover, the bacterial β-gal is an analog to the mammalian senescence-associated β-gal, which is a marker for aged and thus

[1] **Department of Stress Neurobiology and Neurogenetics, Max Planck Institute of Psychiatry, 80804, Munich, Germany;** [2] **Department of Molecular Pharmacology, Albert Einstein College of Medicine, 10461, Bronx, New York;** [3] **Core Unit Neuroimaging, Max Planck Institute of Psychiatry, 80804, Munich, Germany;** [4] **Department of Translational Research in Psychiatry, Max Planck Institute of Psychiatry, 80804, Munich, Germany;** [5] **Institute of Developmental Genetics, Helmholtz Zentrum Muenchen, German Research Center for Environmental Health (GmbH), Ingolstaedter Landstrasse 1, Neuherberg, D-85764, Germany;** [6] **The Solomon H. Snyder Department of Neuroscience, Johns Hopkins University, Baltimore, Maryland;** [7] **Department of Neurogenetics, Max Planck Institute of Experimental Medicine, Goettingen, 37075, Germany**
Grant sponsor: German Federal Ministry of Education and Research; Grant number: FKZ 01ZX1314H.
*Correspondence to: Dr. C.T. Wotjak, Max Planck Institute of Psychiatry Department of Stress Neurobiology and Neurogenetics, Kraepelinstrasse 2- 10 80804 Munich Germany. E-mail: wotjak@mpipsykl.mpg.de
Accepted for publication 8 April 2016.
DOI 10.1002/hipo.22601
Published online 00 Month 2016 in Wiley Online Library (wileyonlinelibrary.com).

functionally deteriorating cells (Dimri et al., 1995; Geng et al., 2010).

The Cre/*loxP* system itself has been previously investigated regarding potential side-effects and has been found to be not always inert (Schmidt-Supprian and Rajewsky, 2007; Giusti et al., 2014a). Similarly, in vitro expression of another reporter protein, namely yellow fluorescent protein (YFP), has been shown to induce neurodegenerative-like effects including altered neuronal morphology (Comley et al., 2011). Although *lacZ* expression is widely used as a constitutively or adult-induced expressed protein marker for the validation and verification of a genetic manipulation (Skarnes et al., 2011; White et al., 2013), as well as a readily detectable tag of plasmid transfection in vitro and in vivo (Crouthamel et al., 2012; Fujikawa et al., 2014; Mota et al., 2014), to the best of our knowledge no study so far has specifically investigated the consequences of *lacZ* expression.

Therefore we here analyzed the consequences of constitutive and adult-induced *lacZ* expression from the Rosa26 locus (Soriano, 1999) in glutamatergic or GABAergic forebrain neurons in mice on a C57Bl/6 genetic background (R26R:Nex-Cre or R26R:Dlx5/6-Cre mice, respectively (Goebbels et al., 2006; Monory et al., 2006)). Animals underwent comprehensive behavioral testing including basal exploratory activity in the open field, anxiety-related behavior in the dark-light box, acoustic startle response as well as cognitive performances regarding contextual fear-conditioning and hippocampus-dependent spatial learning in the water-cross maze (Kleinknecht et al., 2012; Reichel et al., 2015). Additionally, animals underwent in vivo structural analyses via manganese-enhanced magnetic resonance imaging (MEMRI) (Grünecker et al., 2010; Grünecker et al., 2013) and *post mortem* Golgi analyses of dendritic profiles. Moreover, we performed cell viability assays with neuronal cell cultures transfected with a β-gal expressing plasmid. Overall, our data demonstrate that expression of lacZ is not inert to the animals with a particular susceptibility of the hippocampus formation.

MATERIALS AND METHODS

We employed exclusively male mice, aged two to eleven months. Mice were housed individually in type II standard Makrolon cages in a 12 h: 12 h inverse light/dark cycle in a temperature and humidity controlled room at least 10 days prior to behavioral testing (in case of Tamoxifen treatment, mice were singly housed 10 days prior to behavioral testing after Tamoxifen treatment). Mice were granted access to food and water *ad libitum*. Behavioral testing was performed during the dark phase between 9 a.m. and 9 p.m. (i.e., during the activity phase of the animals). Experimental procedures were approved by the Committee on Animal Health and Welfare of the State of Bavaria (Regierung von Oberbayern, Munich, Germany) and were performed in compliance with the European Economic Community (EEC) recommendations for the care and use of laboratory animals (2010/63/EU).

Generation of Transgenic Mouse Lines

lacZ-, *GFP*- and *eYFP*-expression was achieved by employing the Cre/loxP system (Hoess et al., 1982). Mouse lines expressing *lacZ* were generated by breeding homozygous *lacZ*/*lacZ* ROSA26 reporter (R26R) mice (Soriano, 1999) to different heterozygous and hemizygous Cre-driver lines (i.e. Cre+/-). The *lacZ* sequence in the R26R mice is preceded by a STOP sequence flanked by two loxP sites that prevents *lacZ* expression but which is excised upon Cre-recombination. In order to investigate the consequences of *lacZ* expression in cortical glutamatergic neurons, the Nex-Cre driver line (Schwab et al., 1998; Goebbels et al., 2006) was bred to R26R mice (henceforth R26R:Nex-Cre). The Nex-Cre driver line was originally generated by a knock-in of Cre into the Nex locus and was therefore itself employed to control for the heterozygosity of the Nex-locus. Additionally, genuine *lacZ*-expression-effects were subsequently assessed in comparison to GFP expression in glutamatergic cortical neurons, which was achieved by breeding homozygous CAG-CAT-EGFP reporter mice (Nakamura et al., 2006) to the Nex-Cre driver line (CAG-CAT-EGFP:Nex-Cre). Mice selectively expressing ChR2(H134R)-EYFP in forebrain glutamatergic neurons were generated by breeding homozygous Nex-Cre mice to homozygous Ai32 mice ((Madisen et al., 2012) purchased from the Jackson Laboratory; Ai32:Nex-Cre). Glutamatergic *lacZ* expression induced in adulthood was achieved by employing a fusion product of Cre and a variant of the ligand binding domain of the human estrogen receptor (ER^{T2}; (Feil et al., 1997)). Upon Tamoxifen administration the Cre fusion product translocates into the cell nucleus and induces *lacZ* expression (Erdmann et al., 2007). R26R:Nex-Cre-ER^{T2} (henceforth i-R26R:Nex-Cre) (Agarwal et al., 2012) mice received exclusively Tamoxifen-containing food (LASCRdiet^{TM} CreActive TAM400; LASvendi) for three weeks at the age of four months, which reliably induced *lacZ* expression.

GABAergic *lacZ* expression in the forebrain was accomplished by breeding homozygous R26R mice to Dlx5/6-Cre driver mice (R26R:Dlx5/6-Cre) (Monory et al., 2006).

All mice were bred on a C57Bl/6N genetic background for at least 10 generations. Each test group consisted of Cre-positive (Cre+) and Cre-negative (Cre-) littermates. The experimenter was blind to the respective genotypes during behavioral testing and subsequent analyses.

Genotyping

Genotyping was performed as previously described (Refojo et al., 2011). Mouse lines containing reporter sequences (i.e., for *lacZ* or *GFP*) were first genotyped for the respective reporter and then for the specific Cre line.

Following primers were used for R26R: ROSA-1: 5′ AAA GTC GCT CTG AGT TGT TAT 3′, ROSA-2: 5′ GCG AAG AGT TTG TCC TCA ACC 3′, ROSA-5: 5′ TAG AGC TGG TTC GTG GTG TG 3′, ROSA-6: 5′ GCT CAT TAA AAC

CCC AGA TG 3′. These primers resulted in a 398-bp wild-type and a 320-bp mutant Product at standard PCR conditions. A premature deletion of R26R would have been detected by the presence of a 505-bp product.

The presence of Nex-specific Cre was determined by a PCR using the following primers: NexCre 4: 5′ GAG TCC TGG AAT CAG TCT TTT TC 3′, NexCre 5: 5′ AGA ATG TGG AGT AGG GTG AC 3′ and NexCre 6: 5′ CCG CAT AAC CAG TGA AAC AG 3′. Under standard conditions the PCR resulted in a wild-type (i.e. Cre negative) product of 770-bp and a Nex-Cre positive product of 525 bp.

To assess the presence of Dlx-specific Cre, a PCR was performed using the following primers: Dlx-fwd: 5′ CAC GTT GTC ATT GGT GTT AG 3′, Dlx-rev: 5′ CCG GTC ATG ATG TTT TAT CT 3′, Thy1-F1: 5′ TCT GAG TGG CAA AGG ACC TTA GG 3′, Thy1-R1: 5′ CCA CTG GTG AGG TTG AGG 3′. This resulted in a 313 bp product for Dlx-Cre positive samples and a 372 bp control product (Thy1).

R26R:Nex-Cre-ERT2 were again first genotyped for R26R (see above) and the presence of the Nex-Cre-ERT2 fusion product was examined using the following primers: Nex-ORF-as: 5′ AGA ATG TGG AGT AGG GTG AC 3′, Cre-as:5′ CCG CAT AAC CAG TGA AAC AG 3′ and Exon1-s: 5′ GAG TCC TGG AAT CAG TCT TTT TC 3′. Under standard PCR conditions this resulted in a product of ∼ 500 bp for Cre-ERT2 positive samples and a ∼800 bp product for Cre-ERT2 negative samples.

CAG-CAT-EGFP:Nex-Cre mice were first genotyped for their GFP reporter sequence with the following primers: EGFP-fwd: 5′ CCT ACG GCG TGC AGT GCT TCA GC 3′, EGFP-rev: 5′ CGG CGA GCT GCA CGC TGC GTC CTC 3′. The presence of the CAG-CAT-EGFP sequence resulted in a 345 bp product. Subsequently these mice were also genotyped regarding the presence of the Nex-Cre (see above).

Genotyping for ChR2 was performed using the primers Tom1 5′-AAG-GGA-GCT-GCA-GTG-GAG-TA-3′, Tom2 5′-CCG-AAA-ATC-TGT-GGG-AAG-TC-3′, Tom3 5′–GGC-ATT-AAA-GCA-GCG-TAT-CC-3′and Ai32 5′-ACA-TGG-TCC-TGC-TGG-AGT-TC-3′. Standard PCR conditions resulted in a wild-type PCR product of 297-bp and a ChR2-specific PCR product of 212-bp.

Behavioral Testing

Open field

Open Field (OF) testing was performed under red light conditions as described previously (Carola et al., 2002; Jacob et al., 2009; Yen et al., 2013). Animals were placed in an open field box (26 × 26 × 38 cm, Coulbourn Instruments, Allentown, PA, USA) and allowed to explore freely for 30 min. The floor of the box was surrounded by two infrared sensor rings. Infrared beam brakes were recorded and later analyzed as horizontal or vertical movements. The infrared sensors were located 2 and 5 cm above the floor of the box, spaced apart by 1.52 cm and connected to the Tru Scan Software Version 1.1 (Coulbourn Instruments) with a sampling rate of 4 Hz. Each OF box was surrounded by an additional box made of opaque Plexiglas side walls (47 × 47 × 38 cm). After testing, mice were returned to their home cages, and the OF boxes and floor planes were thoroughly cleaned with water and dried.

Movements were scored by the software as follows: if only the lower infrared beams recorded beam-brakes (i.e., all four paws on the floor), the program scored this as horizontal movement/rest; if lower and upper rows of infrared beams recorded beam-brakes, this was scored as vertical movement (e.g., rearing); if only the upper row of beams recorded beam-brakes it was scored as jumping. Total horizontal movement (i.e., distance) was later analyzed in 5 min bins.

Dark-light box

Dark-Light Box testing (DL) was performed as previously described (Jacob et al., 2009). Briefly, the DL box consisted of a dark compartment (15 x 20 x 25 cm) and an illuminated (600 lux) compartment (30 x 20 x 25 cm). These compartments were connected by a 4 cm-long darkened tunnel. Each animal was placed in the dark compartment and then recorded for 5 min. The entire box was thoroughly cleaned between animals with water containing detergent and dried before placing the next animal inside. After testing, latency to enter the light compartment, frequency to enter the light compartment and relative time (duration) spent in the light compartments were analyzed by a trained observer blind to the animals' genotype.

Acoustic startle response

Acoustic Startle Response (ASR) was assessed as previously described (Golub et al., 2009). In brief, mice were placed in a non- restrictive Plexiglas cylinder which was mounted to a plastic platform located in a sound attenuated chamber (SR-LAB, San Diego Instruments SDI, San Diego, CA). A piezoelectric sensor underneath each cylinder enables the quantification of changes in the conductance as a response to varying acoustic stimuli. Startle amplitude was defined as the peak voltage output within the first 50 ms after stimulus onset. The startle stimuli consisted of 20 ms white noise bursts at 75, 90, 105, and 115 dB SPL against a constant background noise of 50 dB SPL. Startle response Input/Output curve was assessed via a protocol consisting of 136 pseudo randomized trials of aforementioned white noise bursts. All cylinders were thoroughly cleaned with water containing detergent between animals. Mean startle amplitude per stimulus intensity was later analyzed in an Input/Output curve.

Fear conditioning

Fear Conditioning (FC) was performed as previously described (Kamprath and Wotjak, 2004). Mice were placed in conditioning chambers (ENV-307A, MED Associates) with elongated Plexiglas walls and a grid floor for shock application. The grid floor was placed above bedding identical to the home cage bedding. The conditioning context was thoroughly cleaned and sprayed with 70% Ethanol (EtOH) between animals. On d0 of the FC protocol mice were placed in the

conditioning context and were allowed to freely explore it for 3 min under house light (0.6 Lux) conditions. Subsequently a 20 s tone (9 kHz at 80 dB SPL) was presented, the last 2 s of which co-terminated with a 0.7 mA foot shock. After shock application mice remained in the conditioning context for an additional 60 s without tone presentation before being placed back to their home cage. The conditioning context was additionally placed in separate sound attenuating isolation boxes.

On d1 (24 h after shock application) mice were placed back in the conditioning context for 3 min under house light conditions without tone or shock presentations and behavior was recorded. Approximately 3 h later mice were placed in a novel context with different contextual features (e.g. cylinder instead of cubicle, bedding without grid, 1% acetic acid (CH_3COOH) instead of EtOH) under house light conditions for 3 min without tone presentation followed directly by a 3 min tone presentation.

After testing, freezing behavior (i.e., immobility except for breathing) was scored by a trained observer blind to the animals' genotype.

Extinction training

Extinction training was performed on Day 2, 3, 4, and 11 after fear conditioning. Mice were placed in a novel environment (cylinder, bedding, 1% acetic acid) for 21 min and were exposed to ten 20 s tone presentations in a semi-random fashion starting at 180 s per day. Freezing response to the first tone presentation per day was later analyzed by a trained observer blind to the animals' genotype as a measure of long-term extinction of the freezing response (Plendl and Wotjak, 2010).

Water cross maze

Water Cross Maze (WCM) training was performed using the hippocampus-dependent place learning protocol as previously described (Kleinknecht et al., 2012; Reichel et al., 2015). The WCM consisted of four arms termed N, E, S and W made of clear Plexiglas. It was filled with water (22°C ± 1°C) up to 12 cm and contained an invisible platform of 10 cm height and 8 x 8 cm surface area at the end of the W arm. Each mouse had to perform 6 starts per day (inter-trial interval: 10 min), alternating between N and S as starting positions in a semi random fashion (if mice were started from N the S arm was closed off, if mice were started from S, the N arm was closed off). Wrong and correct arm entries were recorded manually during WCM training and later translated to Accuracy scores. A trial was deemed "accurate" if the animal swam directly to the platform without entering a wrong arm or returning to the start arm. An animal was deemed "accurate" if it performed at least 5 (out of 6) accurate trials per day (≥ 83.3%). The number of Learners was calculated as the percentage of accurate performers per experimental group per day.

In Vivo Measurement of Hippocampus Volume by Means of Manganese-Enhanced Magnetic Resonance Imaging (MEMRI)

MEMRI was performed as previously described (Grünecker et al., 2010; Kleinknecht et al., 2012; Grünecker et al., 2013). Mice were injected i.p. with a 50 mM $MnCl_2$ solution in 0.9% NaCl at a 30 mg/kg concentration for 8 consecutive days. Subsequently, mice were scanned one day after the last injection with a 7T Avance Biospec scanner (Bruker BioSpin, Ettlingen, Germany). During image acquisition animals were anaesthetized using inhalation anesthesia with an isoflurane–oxygen mixture (1.5–1.9 vol.% isoflurane with an oxygen flow of 1.2–1.4 l/min) and their heads were fixed in a prone position. 3D T_1-weighted and T_2-weighted images were acquired (total measurement duration ∼2 h) and analyzed regarding volumetric differences for several regions of interest (ROIs, e.g., hippocampus, lateral ventricles). 3D MRI images had a spatial resolution of 125 x125 x 140.6 mm^3 and the images were reconstructed using Paravision software (Bruker BioSpin). Further post-processing was performed using SPM (www.fil.ion.ucl.ac.uk/spm). All initial volume data-sets were normalized to their respective whole brain volume. Subsequently, *lacZ*-negative (i.e., normalized values of the test group without *lacZ* expression) mean volume per ROI was defined as 100% and *lacZ*-positive ROI values were calculated in relation to these 100%. For further details regarding image analyses see Grünecker et al. (2010) and Kleinknecht et al. (2012) (Grünecker et al., 2010; Kleinknecht et al., 2012).

X-Gal Staining

Mice were killed by an overdose of isoflurane inhalation and subsequently transcardially perfused with 4% PFA-PBS + 0.005M EGTA + 0.001M $MgCl_2$ at pH = 7.8. Brains were carefully dissected out, and stored in 20% sucrose-PBS + 0.005 M EGTA + 0.001M $MgCl_2$ at 4°C over night. The next day brains were flash-frozen in methylbutane on dry ice and stored at −80°C. Brains were sliced into 40–50 μm Cryostat sections and X-Gal staining was performed as previously described (Weiss et al., 1997; Lu et al., 2008) at the same pH as the perfusion solution.

GFP-Immunofluorescence

Mice were killed by an overdose of isoflurane inhalation and subsequently transcardially perfused with 4% PFA-PBS and post-fixed for one hour in 4% PFA-PBS. Brains were cut on a vibratome into 40 μm sections. Free floating sections were blocked in 10% NGS in 1% Triton- PBS for 2 h and then incubated with the primary antibody (Abcam #ab13970; chicken polyclonal anti- GFP; 1 : 5,000) in 1% NGS- 0.3% Triton- PBS at 4°C over night. Afterwards sections were washed in PBS and then incubated with the secondary antibody (Invitrogen #A-11042, alexa Fluor 594 goat anti- chicken; 1:1,000) in 1% NGS- 0.3% Triton-PBS for 2 h. Last, sections were washed again in PBS and then mounted and covered with mounting medium containing DAPI.

ChR2/eYFP Expression

Mice were killed by an overdose of isoflurane inhalation followed by cervical dislocation. Brains were carefully dissected and flash-frozen in methylbutane on dry ice and stored at −80°C. Subsequently brains were sliced into 30 μm cryostat sections and mounted with Vectashield HardSet Antifade mounting medium with DAPI (Vectorlabs, H-1500-10). 20 − 25 high resolution fluorescence images were taken per brain section using a Zeiss Axioplan 2 epifluorescence microscope and stitched together using the Stitching Fiji ImageJ plugin (Preibisch et al., 2009).

Golgi Staining

Dendrite morphology was assessed by staining the brains of R26R:Nex-Cre^{+} and their wild-type littermates with the FD Rapid GolgiStain^{TM} Kit (FD Neuro Technologies, Columbia, MD) according to the protocol given by the manufacturer. 24 CA1 pyramidal neurons per genotype ($N = 4$ brains per genotype) were traced using a 40x objective lens and the Olympus BX51 microscope with the software Neurolucida 6 (MBF Bioscience, Williston, VT). Sholl analyses and dendritic length were evaluated using the Neurolucida Explorer (MBF Bioscience) (Giusti et al., 2014b).

In Situ Hybridization

ISH was performed as previously described(Lu et al., 2008; Refojo et al., 2011). Nex-Cre mice were anaesthetized with isoflurane and sacrificed by decapitation. Brains were immediately dissected, and shock frozen on dry ice. Frozen brains were cut on a cryostat in 20 μm sections and mounted on SuperFrost Plus slides. For *Cre* mRNA expression analysis, a probe including the nucleotides 112-773 of the GenBank accession number AB449974 was used. Specific riboprobes were generated by PCR applying T7 and SP6 primers using plasmids containing the above mentioned template cDNA. Radiolabeled sense and antisense cRNA probes were generated from the respective PCR products by in vitro transcription with ^{35}S-UTP using T7 and SP6 RNA polymerase. After 20 min of DNase I (Roche) treatment, the probes were purified by the RNeasy-min protocol (Qiagen, Hilden, Germany) and measured in a scintillation counter. The sections were hybridized overnight 57°C with a probe concentration of 7×10^6 c.p.m.ml^{-1}. Subsequently they were washed at 64°C in 0.1 x saline sodium citrate (SSC) and 0.1 mM dithiothreitol. In order to visualize hybridization signals, dried slides were exposed to a special high performance X-ray film (Kodak, BioMax) for different time intervals. For quantification, autoradiographs were digitized and relative levels of mRNA were determined by computer-assisted optical densitometry (ImageJ).

Stereotactic Surgery for AAV Injection

Floxed homozygous R26R mice at the age of 10 weeks were unilaterally injected with PBS ($n = 6$), GFP- AAV (pAAV2.1-sc-GFP-pACG-2-M4; $n = 6$; kindly provided by Dr. Stylianos Michalakis, Dept. Pharmacy LMU Munich) or Cre-AAV (pAAV2.1-CMV-Cre-2A-GFP M4; $n = 6$; kindly provided by Dr. Stylianos Michalakis, Dept. Pharmacy LMU Munich) under deep isoflurane anesthesia and Meloxicam-analgesia. Injection volume was 1 μl per injection side, which were the dorsal (A-P −1.8; L −1.3; V +1.2; from bregma) and ventral left hippocampus (A-P −2.8; L −3.0; V +4.0; from bregma). Preliminary studies had revealed *lacZ* and *GFP* expression present throughout the targeted hippocampus with minimal contralateral spreading 4 weeks after injection. Four months after injection mice underwent the MEMRI procedure.

Cellular Consequences of lacZ *Expression*

Neuro-2a cells were cultivated and subsequently electroporated with a plasmid expressing either *ß*-galactosidase, Gaussia-Luciferase (not secreted mutant) or an empty vector under the CMV promoter in addittion to a GFP-expressing construct for normalization to transfection efficacy (Perisic et al., 2010; Schumann Burkard et al., 2011; Gassen et al., 2014).

Statistical Analyses

Data were analyzed blind to the genotype of the animals by means of parametric (t-test or ANOVA followed by Tukey HSD post-hoc test if appropriate and as indicated in the text) or distribution (chi^2) statistics using STATISTICA for Windows (V 5.0 StatSoft, Inc., 1995), GraphPad Prism^{TM} (version 5.0; GraphPad Software Inc.; San Diego, CA) or SPSS 16.0. Results were considered significant if $P \leq 0.05$. All results were plotted with GraphPad Prism^{TM} (version 5.0; GraphPad Software Inc.; San Diego, CA) as mean ± standard error of mean (SEM).

RESULTS

Behavioral and Structural Consequences of lacZ Expression in Cortical Glutamatergic Neurons

Given the prevalence of glutamatergic neurons throughout the CNS and their strong implication in several behavior traits, we first investigated the constitutive expression of *lacZ* in glutamatergic neurons of the cerebral cortex. We bred the Nex-Cre driver line to R26R mice (henceforth R26R:Nex-Cre), and compared Cre-positive and thus *lacZ* expressing offspring to their Cre-negative littermates (Bartholomä and Nave, 1994; Akagi et al., 1997; Schwab et al., 1998; Goebbels et al., 2006). Visualization of *lacZ* expression by X-Gal staining for R26R:Nex-Cre^{+} mice illustrated a strong expression pattern throughout the cortical layers, the hippocampus and the basolateral amygdala (Fig. 1a). Behavioral testing of these mice at the age of four months revealed a markedly increased locomotor activity in the open field (OF; Fig. 1b; ANOVA: $F_{1,17} = 10.64$, $P = 0.0046$) and decreased anxiety-related

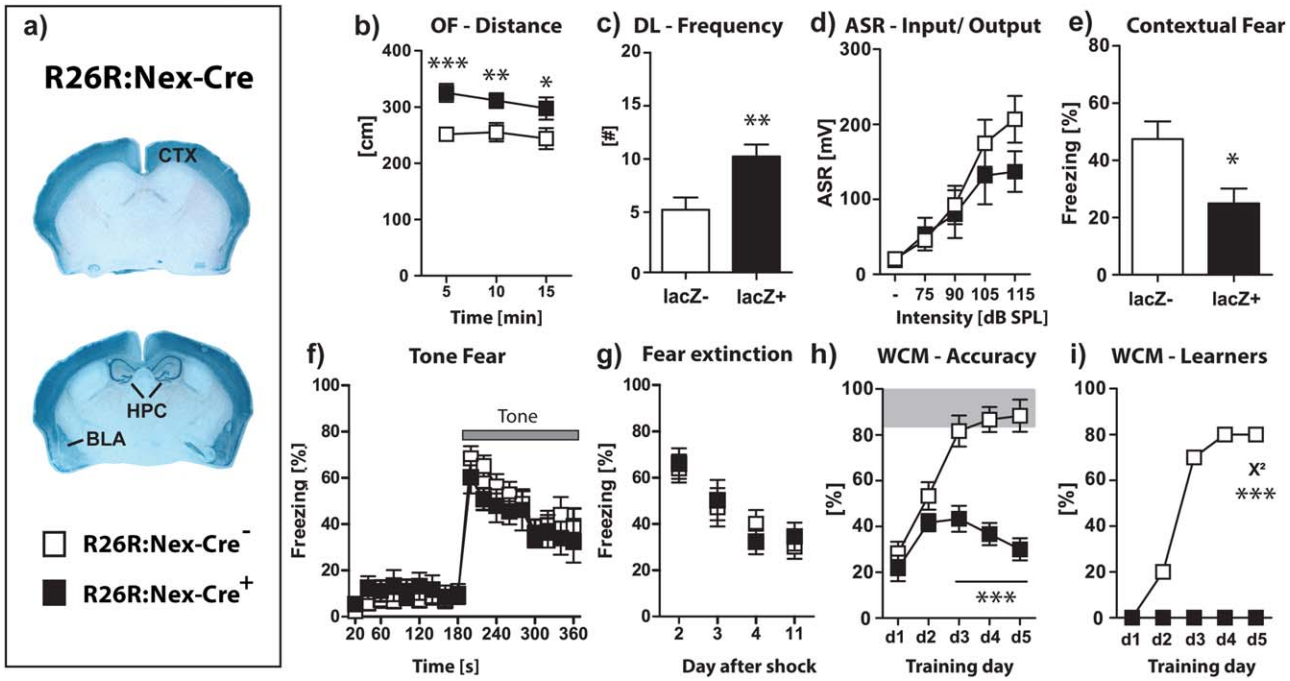

FIGURE 1. Behavioral consequences of *lacZ* expression in cortical glutamatergic neurons. (a) X-Gal staining for R26R:Nex-Cre$^+$ mice revealed strong expression in the cortex (Ctx), hippocampus (HPC) and basolateral amygdala (BLA); (b) locomotor activity assessed as distance traveled in the open field; (c) anxiety-related behavior assessed by frequency to enter the light compartment in the dark-light box; (d) arousal levels assessed by acoustic startle responses; (e) contextual fear shown upon a 3-min re-exposure to the conditioning context 24 h after conditioning; (f) expression of auditory-cued fear 24h after conditioning; (g) freezing response to the first tone presentation per day over the course of extinction training (i.e., mice were exposed to ten 20-s tones per day on Days 2, 3, 4, and 11 after conditioning); (h) spatial learning reflected by accuracy levels for WCM performance (i.e. percentage of correct trials per day); (i) number of accurate learners in the WCM per group and training day. Mean ± SEM; *$P < 0.05$, ** $P < 0.01$, *** $P < 0.001$ vs. R26R:Nex-Cre$^-$ littermate controls, i.e. mice without *lacZ* expression (Student's *t*-test, χ^2 test or ANOVA followed by Tukey HSD post hoc test). ASR, acoustic startle response; DL, dark-light box; I/O, input/output; OF, open field; WCM, water cross maze. Behavioral testing was performed with 9 − 10 mice per genotype at the age of 4 − 5 months. [Color figure can be viewed in the online issue, which is available at wileyonlinelibrary.com.]

behavior in the dark-light box (DL; Fig. 1c; unpaired *t*-test: $P = 0.0066$), but no changes regarding acoustic startle response (ASR), compared to R26R:Nex-Cre$^-$ littermate controls (Fig. 1d). Moreover, R26R:Nex-Cre$^+$ mice presented with severe impairments in hippocampus-dependent learning tasks as illustrated by a significantly decreased contextual fear memory 24 h after shock application (Fig. 1e; unpaired *t*-test: $P = 0.0138$).

Despite this marked impairment regarding contextual fear memory, glutamatergic *lacZ* expression did not affect acquisition, expression and long-term extinction of auditory-cued fear memory (Figs. 1f,g). This precludes that alterations in pain perception or expression of freezing due to hyperactivity rather than hippocampal processing account for the impairment in contextual fear. In line with a primarily hippocampus-based phenotype, *lacZ* expression completely abolished hippocampus-dependent spatial learning abilities (Fig. 1h; ANOVA Accuracy: $F_{1,18} = 73.2$, $P < 0.0001$), with none of the mutant mice reaching the accuracy criterion in the end of training (Fig. 1i; χ^2, $P < 0.001$).

The severe impairment in hippocampus-dependent memory coincided with a 30% reduction in hippocampal volume and a 2.5-fold increase in lateral ventricle volume (Fig. 2; unpaired *t*-test: $P < 0.0001$), as assessed in vivo by means of manganese-enhanced magnetic resonance imaging (MEMRI) immediately following behavioral testing. To investigate these severe structural deficits more closely, we subsequently performed Golgi staining for R26R:Nex-Cre$^+$ and R26R:Nex-Cre$^-$ littermate controls (Vyas et al., 2002) (Fig. 3). Golgi-Sholl analysis revealed a significantly decreased number of intersections per Sholl-circle (i.e. concentric circles radiating from the cell soma) for CA1 pyramidal neurons of R26R:Nex-Cre$^+$ mice expressing *lacZ* in glutamatergic neurons compared to littermate controls (Fig. 3c; ANOVA genotype: $F_{1,43} = 6.71$, $P = 0.0097$) across the entire neurite tree. Analysis of the total dendritic length for both groups revealed a strong trend towards decreased dendritic length in the hippocampus of R26R:Nex-Cre$^+$ mice (Fig. 3d; unpaired *t*-test: $P = 0.075$). Furthermore, the quantification of the number of dendritic branches per bifurcation order revealed that CA1 neurons of wild type littermates bifurcate up to 25 times, whereas the maximum bifurcation of *lacZ* expressing mice is 20 (Fig. 3e). Of note is the diversity of appearance of CA1 pyramidal neurons of R26R:Nex-Cre$^+$ mice (Fig. 3b, bottom row), indicating that not all neurons might be affected to the same extent.

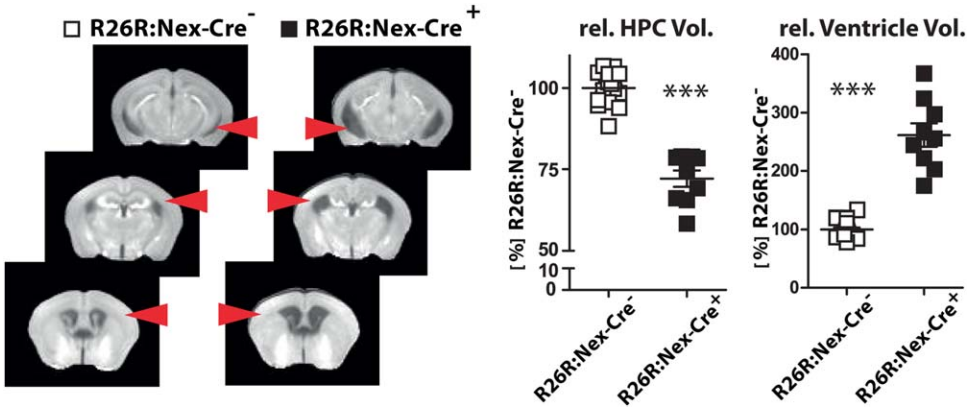

FIGURE 2. Gross morphological changes due to glutamatergic *lacZ* expression. Composite in vivo manganese-enhanced magnetic resonance images (MEMRI) for R26R:Nex-Cre$^-$ and R26R:Nex-Cre$^+$ mice and quantification of hippocampal (HPC) and lateral ventricle volume (arrow heads) normalized to total brain volume. Open symbols represent mice without *lacZ* expression, black symbols represent mice with constitutive *lacZ* cortical glutamatergic expression. Individual data were overlaid with mean ± SEM; *** $P < 0.001$ (Student's t-test). MEMRI was performed at the age of 5 − 6 months. [Color figure can be viewed in the online issue, which is available at wileyonlinelibrary.com.]

Specificity of lacZ Effects

We achieved glutamatergic *lacZ* expression by breeding the glutamatergic Cre-driver line (Nex-Cre) to R26R mice (see above). While originally generating the Nex-Cre driver line, the Cre-recombinase was knocked into the Nex gene locus, which was thereby disrupted (Schwab et al., 1998; Goebbels et al., 2006). To exclude that the severe behavioral and structural phenotype observed in R26R:Nex-Cre$^+$ mice simply resulted from heterozygousity of the Nex locus, we compared behavioral performance and brain morphology of Nex-Cre$^+$ and Nex-Cre$^-$ littermates. We found no behavioral differences between Nex-Cre$^+$ and Nex-Cre$^-$ littermates for OF and WCM performance (Figs. 4a–c), and no differences in hippocampus volume (97.2 ± 2.2% vs. 100.0 ± 1.5%, $P = 0.322$; $n = 7$ and 14).

In order to assess whether the expression of another reporter-protein in cortical glutamatergic neurons would yield similar consequences as observed for *lacZ*, we additionally analyzed mice which express GFP in glutamatergic cortical neurons under the Nex-promoter (CAG-CAT-EGFP:Nex-Cre$^+$ (Nakamura et al., 2006)). Again, GFP expression (Fig. 4d) did not cause any behavioral differences in these mice compared to their non-GFP expressing littermates (Fig. 4e,f; statistics not shown), and no alterations in hippocampus volume (98.0 ± 1.5% vs. 100.0 ± 1.8%, $P = 0.410$; $n = 11$ and 10).

Lastly, expression of the channelrhodopsin 2/eYFP fusion product from the R26R locus on the same genetic background as the R26R:Nex-Cre mice [Ai32:Nex-Cre mice (Madisen et al., 2012)] did not result in spatial learning impairments either. Other than R26R:Nex-Cre$^+$ mice, Ai32:Nex-Cre mice reached the same level of accuracy as R26R:Nex-Cre$^-$ controls (Figs. 4g–i).

Together, these control experiments demonstrate that the alterations in behavior and brain morphology observed for R26R:Nex-Cre$^+$ mice are directly related to the expression of the *lacZ* gene.

Behavioral Consequences of lacZ Expression in GABAergic Neurons

We next asked whether detrimental effects of *lacZ* expression are confined to cortical glutamatergic neurons. To answer this question, we analyzed the consequences of *lacZ* expression in GABAergic forebrain neurons (R26R:Dlx5/6-Cre$^+$). X-Gal staining revealed a strong *lacZ*-expression, among others, for the striatum and the ventral tegmental area (Fig. 5a). At behavioral level, R26R:Dlx5/6-Cre$^+$ displayed an increased locomotor activity in the OF (Fig. 5b; ANOVA: $F_{1,14} = 14.57$, $P = 0.0019$) and decreased anxiety-related behavior in the DL (Fig. 5c; unpaired *t*-test: $P = 0.0335$) compared to R26R:Dlx5/6-Cre$^-$ littermate controls, which resembles the phenotype of R26R:Nex-Cre$^+$ mice (cf. Figs. 1b,c). However, other than glutamatergic *lacZ* expression, expression of *lacZ* in GABAergic neurons led to decreased acoustic startle responses (ASR; Fig. 5d; ANOVA: $F_{1,14} = 5.43$, $P = 0.0353$), while leaving contextual fear memory unaffected (Fig. 5e) and merely slightly impairing hippocampus-dependent spatial learning abilities (Figs. 5f,g; ANOVA *Accuracy*: $F_{1,14} = 5.15$, $P = 0.0396$). Moreover, R26R:Nex-Cre$^+$ mice showed no alterations in hippocampus volume compared to R26R:Dlx5/6-Cre$^-$ littermate controls (97.8 ± 1.7% vs. 100.0 ± 1.7%, $P = 0.387$; $n = 8$ and 9).

We conclude from these experiments that the impact of *lacZ* expression on behavior and brain morphology depend on the targeted neuronal population.

Consequences of lacZ Expression in Adult Animals

Given that the Nex and Dlx5/6 promoters are active at early prenatal stages [E16 and E13 respectively (Schwab et al., 1998; Stühmer et al., 2002)], we conceded the possibility that

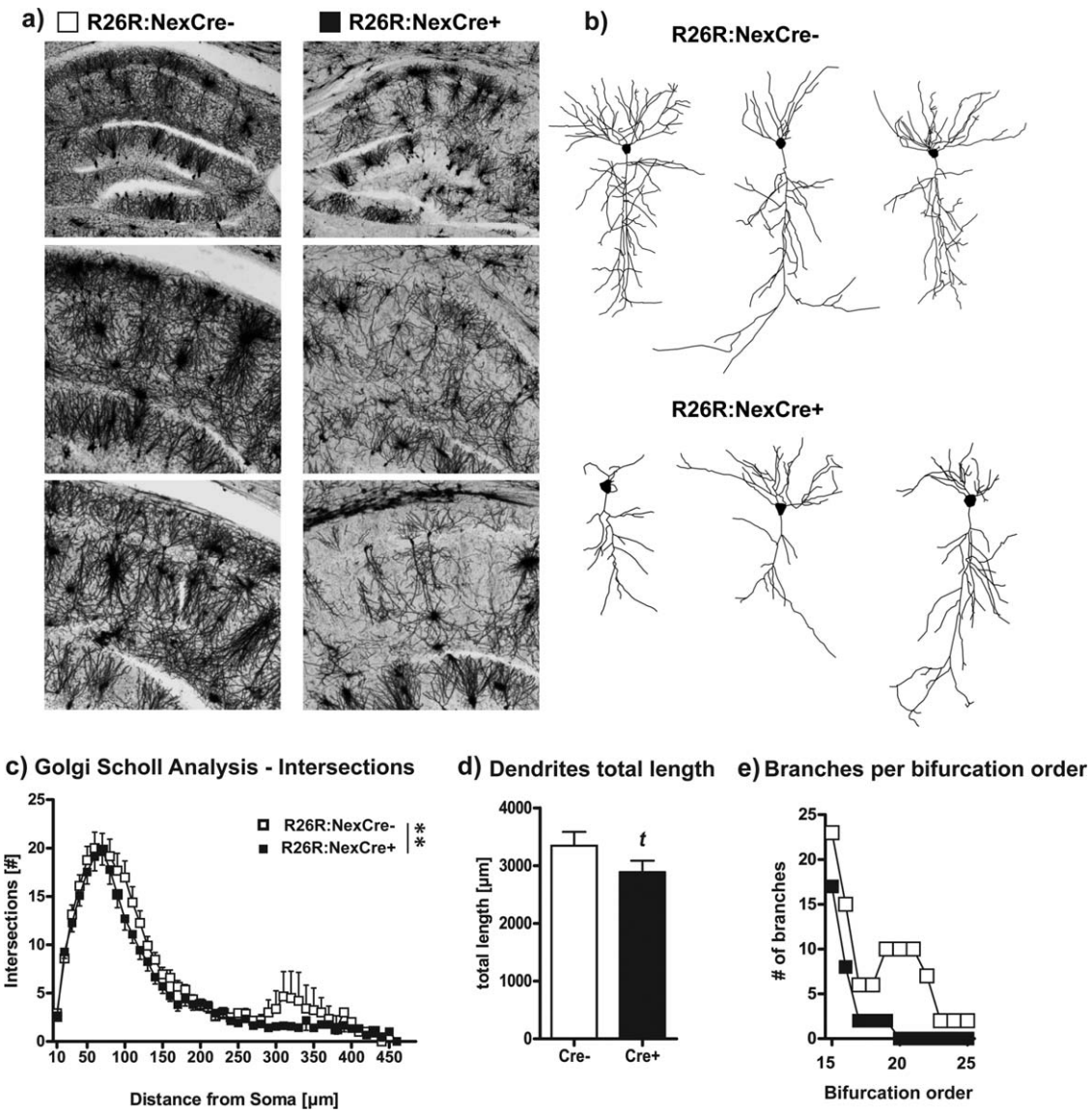

FIGURE 3. Dendritic morphology alterations following glutamatergic *lacZ* expression. (a) representative images of Golgi-stained hippocampi of R26R:Nex-Cre$^-$ (left) and R26R:Nex-Cre$^+$ (right) mice; (b) representative tracings of single CA1 pyramidal neurons from the CA1 region of R26R:Nex-Cre$^-$ (top) and R26R:Nex-Cre$^+$ (bottom) mice (note the broad variance in neuronal morphology in R26R:Nex-Cre$^+$ mice); (c) Golgi Sholl Analysis of the number of intersections with respect to the distance from the soma; (d) total dendritic length; (e) number of branches per bifurcation order. Mean ± SEM; ** $P < 0.01$, (Student's *t*-test or ANOVA followed by Tukey HSD post hoc test). *t* = trend ($P = 0.075$). Brains were collected at the age of 4 − 5 months (sample sizes: R26R:Nex-Cre$^+$ mice = 23 neurons from 4 animals; R26R:Nex-Cre$^-$ mice: 24 neurons from 4 animals).

the detrimental effects observed following glutamatergic or GABAergic *lacZ* expression might be caused by an interaction of *lacZ* expression and embryonic development. Therefore we asked whether the structural deficits observed in R26R:Nex-Cre$^+$ mice could also be induced in vivo in adult mice. We investigated this by unilaterally injecting Cre-encoding adeno-associated viruses (AAV) into the left hippocampus of 10 weeks old homozygous R26R mice (Fig. 6a), and subsequently analyzed changes in brain morphology by MEMRI. We found that unilateral *lacZ* expression led to a significant volume reduction in the transfected side four months after induction compared to the contralateral, non-injected side (Fig. 6d; paired *t*-test: $P < 0.01$). Neither unilateral PBS treatment nor unilateral application of a GFP encoding AAV had similar consequences (Figs. 6b,c; paired *t*-test: $P > 0.110$). Therefore, the reduced hippocampal volume observed for R26R:Nex-Cre$^+$ mice cannot be solely ascribed to developmental effects.

This conclusion was further substantiated by analysis of behavioral and structural consequences of adult-induced *lacZ* expression in glutamatergic cortical neurons, employing tamoxifen-induced *lacZ* expression in adult R26R:Nex-Cre-ERT2 (i-R26R:Nex-Cre) mice (Agarwal et al., 2012). In these animals, Cre expression is driven by the same glutamatergic promoter as

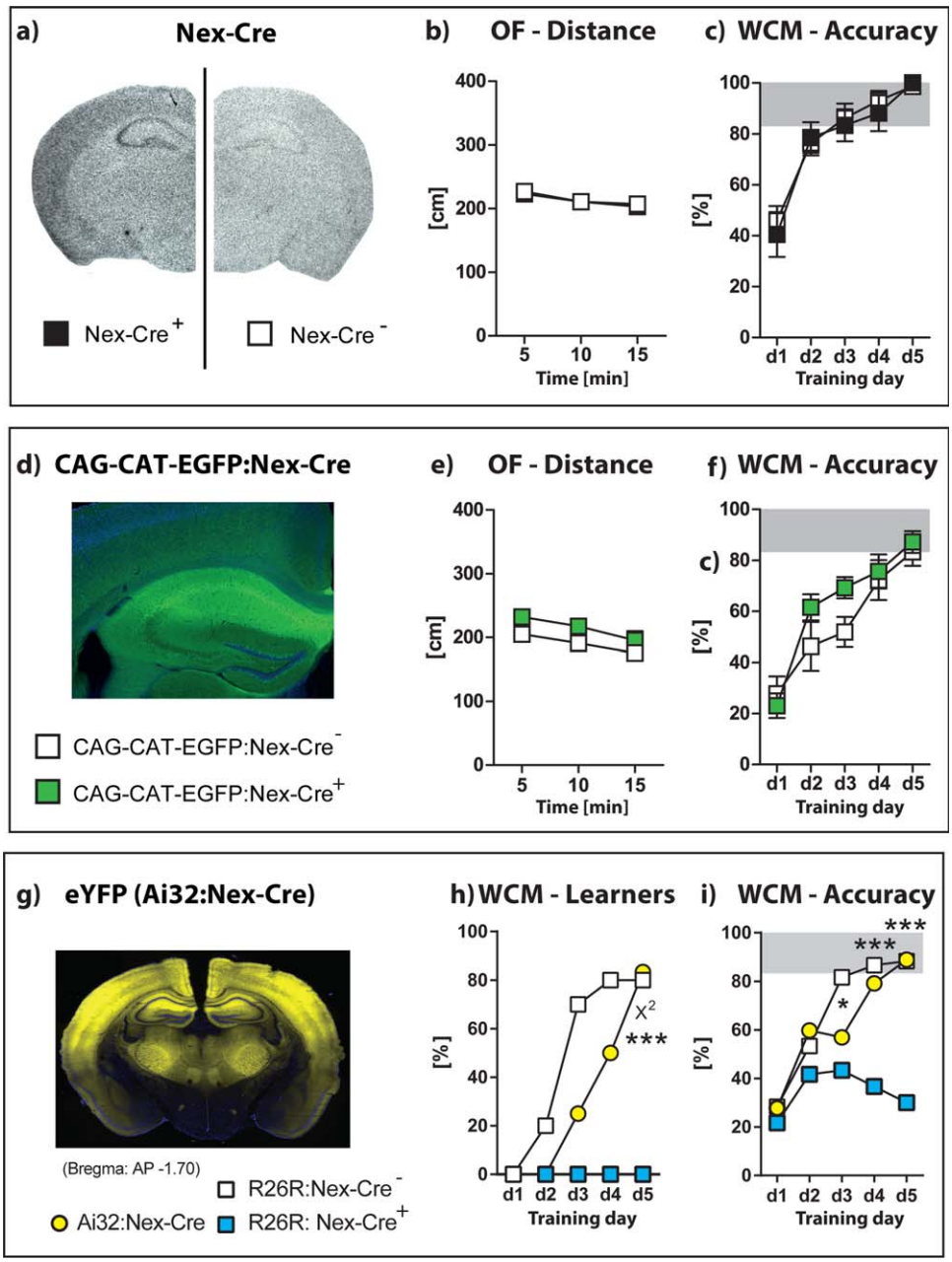

FIGURE 4. Glutamatergic expression of Cre-recombinase, GFP or ChR2/YFP has no behavioral consequences. (a) in situ hybridization showing Cre-recombinase expression in Nex-Cre$^+$ (i.e., with Cre-recombinase; $n = 7$) and Nex-Cre$^-$ (i.e., without Cre-recombinase; $n = 12$) mice. There were no genotype differences in (b) locomotor activity (assessed by distance traveled in the open field) and (c) spatial learning (reflected by accuracy levels in the water cross-maze). (d) Immunofluorescence staining for GFP-expression in the hippocampus of CAG-CAT-EGFP:Nex-Cre$^+$ mice (i.e., with GFP expression; $n = 10$) and CAG-CAT-EGFP:Nex-Cre$^-$ littermate controls (i.e., no GFP expression; $n = 10$). Again, there were no genotype differences in (e) distance traveled in the OF and (f) spatial learning. (g) Expression of the channelrhodopsin 2-eYFP fusion product from the Rosa26 locus in cortical glutamatergic neurons (Ai32:Nex-Cre; $n = 12$). (h,i) Other than R26R:Nex+, Ai32:Nex-Cre reached the same accuracy levels in spatial learning in the water cross-maze as R26R:Nex-Cre- (note that behavioral data of R26R:Nex-Cre- and R26R:Nex-Cre+ are the same as those shown in Fig. 1). Mean ± SEM. * $P < 0.05$ Ai32:Nex-Cre vs. R26R:Nex-Cre$^-$.; *** $P < 0.001$ Ai32:Nex-Cre vs. R26R:Nex-Cre$^+$ (ANOVA followed by Bonferroni post hoc test or X^2 test). OF, open field; WCM, water cross maze. Behavioral testing was performed at the age of 4 − 5 (a−c and d−f) or 7 − 9 months (g−i). [Color figure can be viewed in the online issue, which is available at wileyonlinelibrary.com.]

used for constitutive glutamatergic *lacZ* expression (cf. Figs. 1–3), however only after treatment with tamoxifen. The animals underwent a short behavioral screen (open field and acoustic startle response) before tamoxifen treatment at the age of 3 months, and underwent an extended behavioral screen in parallel to the previous groups 4 months after *lacZ* expression was induced (Fig. 7a). We

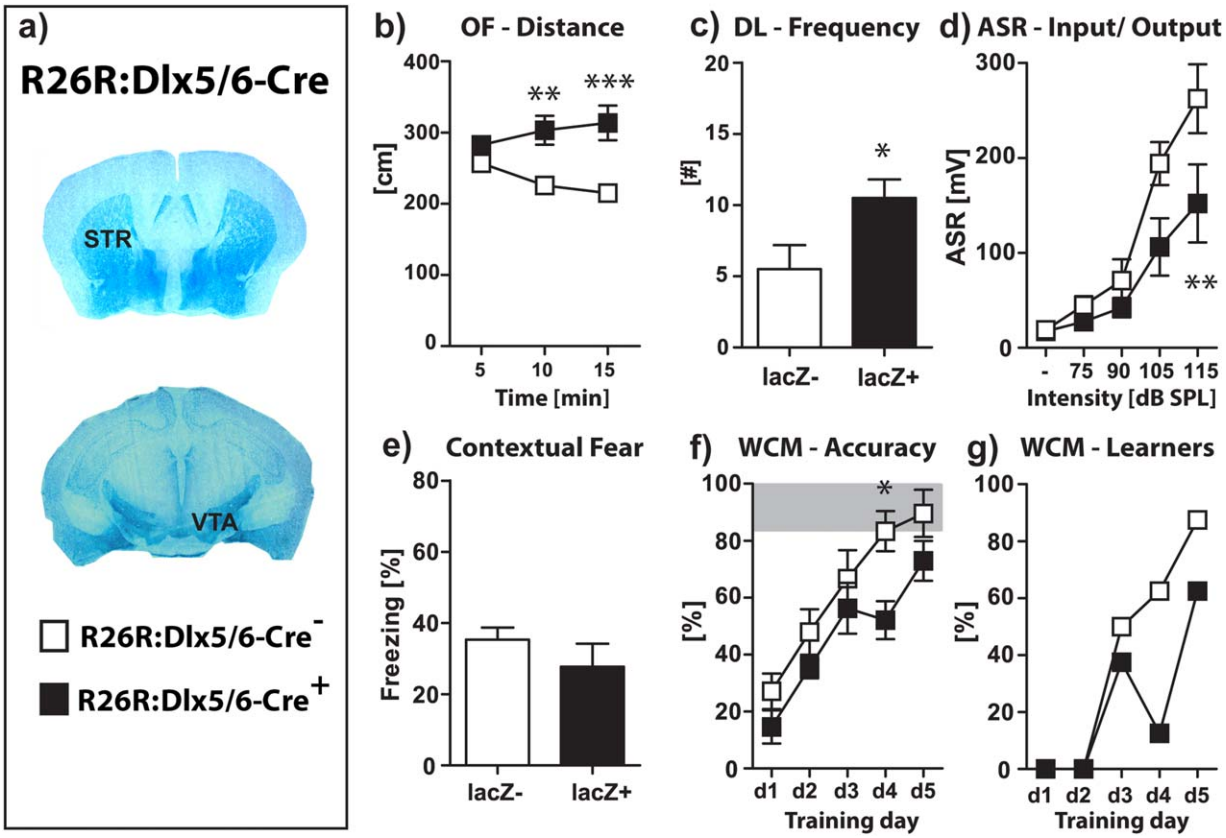

FIGURE 5. Behavioral consequences of GABAergic *lacZ* expression. (a) X-Gal stainings for R26R:Dlx5/6-Cre^{+} mice revealed strong expression pattern for instance in striatum (STR) and ventral tegmental area (VTA); (b) locomotor activity in the open field; (c) anxiety-like behavior in the dark-light box; (d) acoustic startle responses; (e) contextual fear memory 24 h after conditioning; (f) spatial learning reflected by accuracy levels for WCM performance (i.e., percentage of correct trials per day); (g) number of accurate learners in the WCM per group and training day. Mean ± SEM; *$P<0.05$, ** $P<0.01$, *** $P<0.001$ vs. R26R:Dlx5/6-Cre^{-} littermate controls, i.e., mice without *lacZ* expression (Student's *t*-test, χ^2 test or ANOVA followed by Tukey HSD post hoc test). For further details see legend of Fig. 1. Behavioral testing was performed with 8 mice per genotype at the age of 4 − 5 months. [Color figure can be viewed in the online issue, which is available at wileyonlinelibrary.com.]

did not observe any genotype-dependent behavioral phenotype before tamoxifen treatment (data not shown). After tamoxifen treatment, X-Gal staining revealed *lacZ*-expression throughout hippocampus and cortex (Fig. 7a), which was, however, markedly reduced compared to constitutive glutamatergic *lacZ* expression (cf. Fig.1b). Nonetheless, i-R26R:Nex-Cre^{+} showed significant behavioral alterations compared to tamoxifen treated i-R26R:Nex-Cre^{-} littermate controls that—at least in part—correspond to the behavioral and morphological changes observed following constitutive glutamatergic *lacZ* expression (cf. Figs. 1 and 2): Although adult-induced *lacZ* expression did not affect locomotor behavior (Fig. 7b) and spatial learning (Fig. 7f), it led to a decrease in anxiety-related behavior (Fig. 7c; unpaired *t*-test: $P = 0.0437$), contextual fear (Fig. 7e; unpaired *t*-test: $P = 0.0147$) and hippocampal volume (Fig. 7g; unpaired *t*-test: $P = 0.0053$).

LacZ Expression and Neuronal Survival

Expression of *lacZ* in adulthood resulted in a 10 − 12% reduction of hippocampus volume (cf. Figs. 6d and 7g). This reduction is still larger than implied by the Golgi analysis (cf. Fig. 3). Therefore, to assess whether *lacZ* expression affects not only the morphology, but also the survival of neurons, we transfected Neuro-2a cells with a plasmid either expressing ß-galactosidase, Luciferase or an empty vector under the CMV promoter and performed MTT and LDH cell viability assays (Perisic et al., 2010; Schumann Burkard et al., 2011; Zschocke et al., 2011; Gassen et al., 2014). Both assays revealed a highly significant reduction in viability of cells transfected with ß-galactosidase (Figs. 8a,b; MTT, 1-way-ANOVA: $P < 0.0001$; LDH, 1-way-ANOVA: $P = 0.0446$). Thus, decreased neuronal survival may contribute to the volume reduction of the hippocampus observe upon *lacZ* expression.

DISCUSSION

We demonstrate for the first time that *lacZ* expression in vivo is not inert, but causes severe and distinct phenotypic

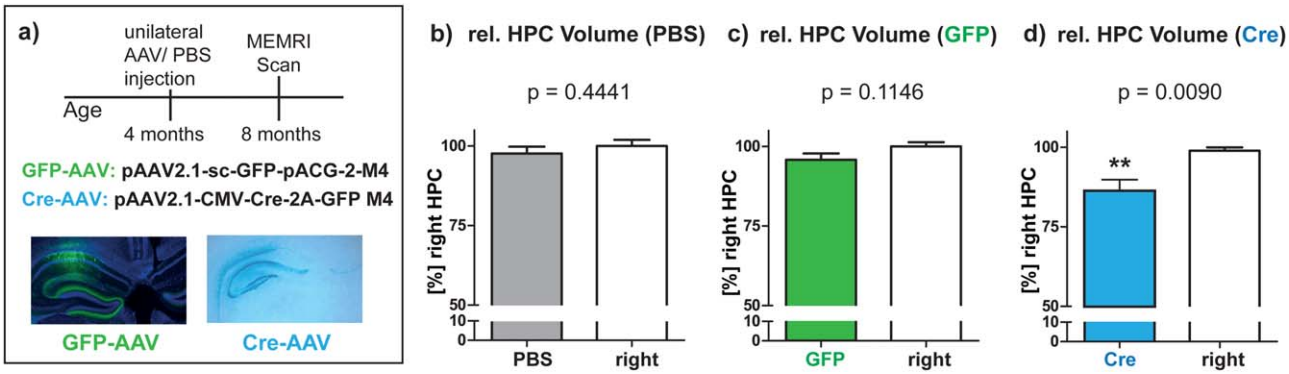

FIGURE 6. Unilateral Cre-AAV induced hippocampal volume loss in adult R26 reporter mice. (a) timeline for unilateral AAV/ PBS injection into the left hippocampus (HPC) of R26R mice and X-Gal/GFP-IF staining 4 weeks after respective AAV injections reveal *lacZ*/GFP expression throughout the targeted HPC; (b−d) MEMRI results of the treated left hippocampus (filled bars) in relation to the untreated right hippocampus (white bars); (b) HPC volume 4 months after PBS injection ($n = 5$); (c) HPC volume 4 months after GFP-AAV injection ($n = 6$); (d) HPC volume 4 months after Cre-AAV injection ($n = 5$). Mean ± SEM; ** $P < 0.01$ (paired Student's t-test). Mice were 3 − 4 months of age at initial AAV injection. [Color figure can be viewed in the online issue, which is available at wileyonlinelibrary.com.]

alterations depending on the affected neuronal population. If *lacZ* was constitutively expressed in cortical glutamatergic neurons, consequences ranged from alterations in anxiety-like behavior and severe impairments in hippocampus-dependent memory to massive volume loss of the hippocampus formation up to ultrastructural changes. These effects were confined to the expression of *lacZ*, since they could not be observed upon expression of GFP, YFP, or Cre-recombinase alone. Furthermore, adult-induced *lacZ* expression in cortical glutamatergic neurons also causes significant, albeit attenuated, behavioral and structural alterations.

The accumulation of proteins and its consequences on neuronal functionality has been the focus of many neurodegenerative disease-related studies (Chishti et al., 2001; Hardy and Selkoe, 2002; Dauer and Przedborski, 2003; Ross and Tabrizi, 2011; Cohen et al., 2013). Additionally, several studies have already reported Cre-mediated side-effects (Schmidt-Supprian and Rajewsky, 2007; Giusti et al., 2014a), yet, to the best of our knowledge, the possibility of detrimental consequences of lacZ expression has not been considered so far. Therefore, we here analyzed the consequences of lacZ expression for two opposing neuronal sub-populations in the mouse forebrain, cortical glutamatergic and GABAergic neurons. We found that lacZ expression is not inert and rather drastically and distinctly affects the phenotype of the animals, depending on the affected neuronal populations. lacZ-induced loss of hepatocytes has been described before and was linked to an immune response (Akagi et al., 1997). Our attempt to identify the origin of the observed 30% hippocampal reduction following constitutive glutamatergic lacZ expression via Golgi analysis revealed only a minor effect of a decreased total dendritic length, but a robust effect regarding a decreased number of intersections for lacZ expressing pyramidal CA1 neurons. This finding indicates a decreased dendritic arborization following lacZ expression and thus could at least partially account for the observed volume loss. Additionally, given the observed decreased cell viability of neurons in culture following transfection with lacZ-coding plasmids, the total neuron number in the HPC of i-R26R:Nex-Cre$^+$ mice might also be reduced. However, as has been shown previously, significant changes in hippocampal volume may not necessarily result from neuronal cell loss, but can be due to multiple mechanisms, including alterations in dendritic arborization and axonal projections (Kassem et al., 2013).

Regarding a possible developmental interaction between *lacZ* expression and embryogenesis, we found that adult-induced *lacZ* expression also caused hippocampal volume reduction, both for AAV-mediated as well as for tamoxifen-induced expression; thus underlining the *lacZ*-driven specificity of the observed effects. Of note, while we did not observe structural or cognitive deficits in our Nex-Cre$^+$ control mice, it has recently been shown that the disruption of the Nex gene locus may result in alterations of anxiety-related behavior (Guggenhuber et al., 2016). Thus, although we cannot exclude cumulative negative effects of a disrupted Nex gene and the *lacZ* expression, due to the numerous control lines used, we feel confident that the marked structural changes and cognitive deficits observed for the R26R:Nex-Cre$^+$ mice are mainly driven by *lacZ* expression. The differential distribution of glutamatergic and GABAergic neurons throughout the hippocampus accounts for the diverging structural consequences of *lacZ* expression between R26R:Nex-Cre$^+$ and R26R:Dlx-Cre$^+$ mice, as there are approximately ten-times more glutamatergic than GABAergic neurons present in the dorsal hippocampus (Jinno and Kosaka, 2010). The extreme volume decrease and general damage of the hippocampus due to glutamatergic *lacZ* expression then also accounts for the severe cognitive impairments observed for hippocampus-based learning paradigms (Sweatt, 2004; Kleinknecht et al., 2012). Interestingly, the markedly reduced *lacZ*-expression pattern for adult-inducible i-R26R:Nex-Cre$^+$ mice compared to the constitutive *lacZ*

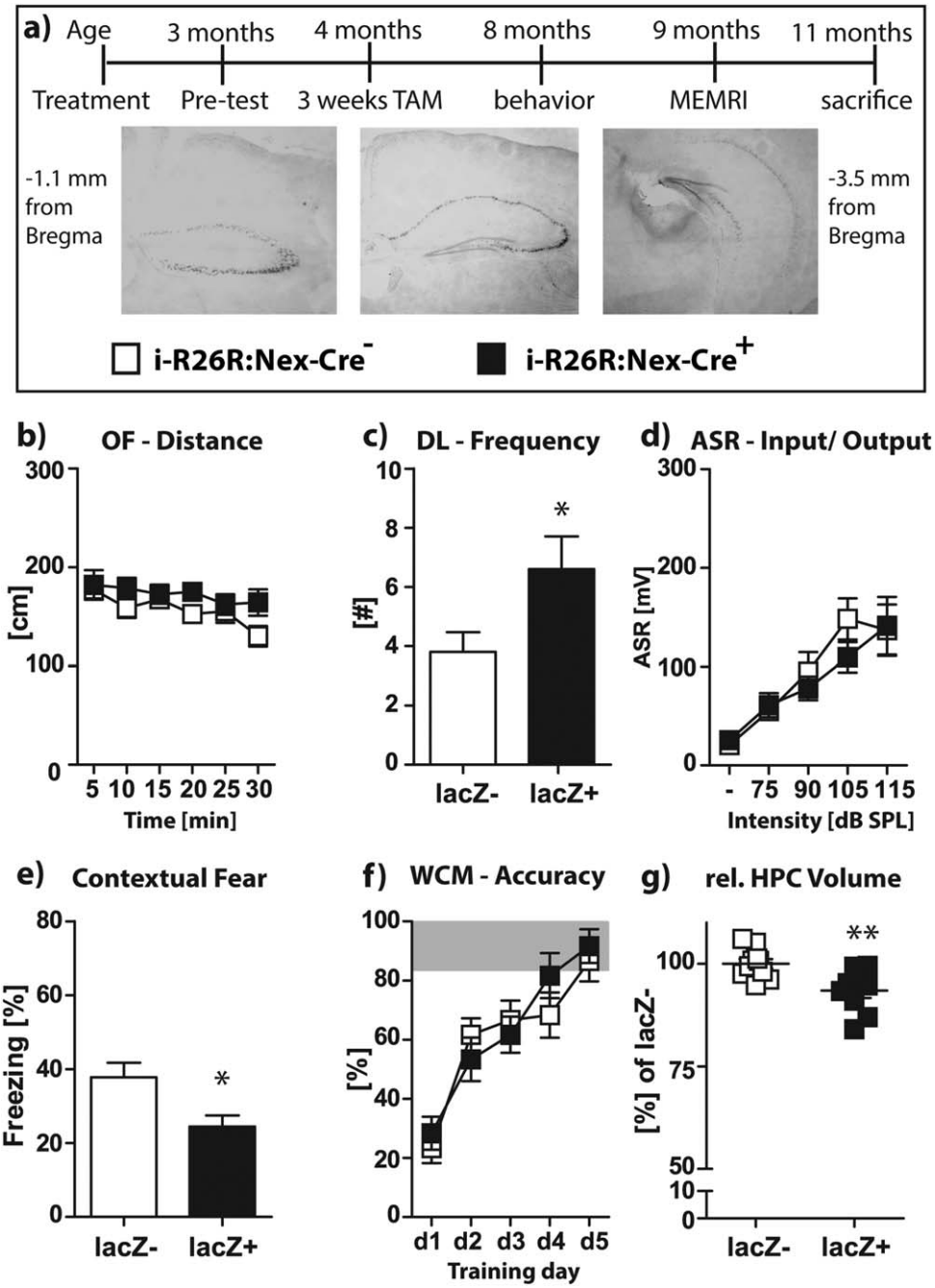

FIGURE 7. Consequences of adult-induced *lacZ* expression in cortical glutamatergic neurons. (a) top: timeline; middle: X- Gal stainings for i-R26R:Nex-Cre^{+} mice revealed reduced expression pattern throughout HPC and cortex 5 months after tamoxifen treatment; (b) locomotor activity in the open field; (c) anxiety-like behavior in the dark-light box; (d) acoustic startle responses; (e) contextual fear memory 24h after conditioning; (f) spatial learning in the WCM; (g) relative hippocampus volume as assessed by MEMRI. Mean ± SEM; * $P < 0.05$, ** $P < 0.01$ vs. tamoxifen treated i-R26R:Nex-Cre^{-} littermate controls (Student's t-test). For further details see legend of Fig. 1. Mice ($n = 9 - 10$ per genotype) were tested and scanned $4 - 5$ months after tamoxifen treatment (i.e., at the age of $8 - 9$ months).

expression (cf. Figs. 1a vs. 7a), as visualized by X-Gal staining, nonetheless resulted in significant behavioral and structural alterations. These findings highlight the possible ramifications of *lacZ* expression, even after a shortened expression-duration and limited expression volume.

Although GFP-related toxicity has been previously reported (Ciesielska et al., 2013), we did not observe any phenotypic alterations following glutamatergic GFP expression or expression of the channelrhodopsin 2-eYFP fusion product and would thus suggest the use of GFP or eYFP rather than *lacZ* as

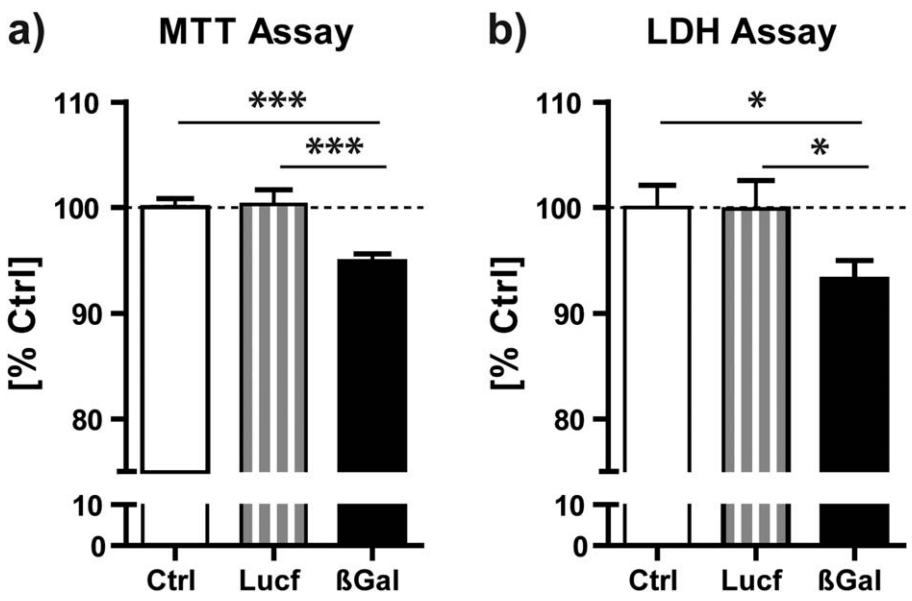

FIGURE 8. Consequences of *lacZ* expression in neuronal cell cultures (neuro-2a cells). (a) MTT cell viability assay normalized to empty vector (Ctrl) viability; (b) LDH cell viability assay normalized to empty vector (Ctrl) viability. Mean ± SEM; * $P < 0.05$, *** $P < 0.001$ (1-ay-ANOVA followed by Student's *t*-test). Ctrl, empty vector control plasmid ($n = 96/64$); Lucf, Luciferase expressing vector ($n = 58/58$); ßGal, ß-galactosidase expressing vector ($n = 96/64$).

reporter proteins for future studies. Given the increasing possibilities of genetic manipulations also for rats and primates, as well as the wide-spread use of *lacZ* as a reporter-protein (Li et al., 2008; Tong et al., 2010; Diester et al., 2011; Skarnes et al., 2011; Witten et al., 2011; Schönig et al., 2012; White et al., 2013) as well as for the Daun02 method (Koya et al., 2009), we urge that reported effects are carefully controlled and that *lacZ* expression will be taken in to account as a contributing factor for any observed phenotypes.

In conclusion, we here demonstrated that *lacZ* expression in different neuronal subpopulations is not inert to the behavioral or structural phenotype of mice, whether expressed constitutively or induced in adulthood or transfected in vitro. Consequently, our results warrant a strong caveat against the (co-) expression of *lacZ* in vitro or in behavioral and structural screening studies, in particular in respect to hippocampus-dependent processes.

Acknowledgments

The authors gratefully acknowledge the help of Dr. S. Giusti and Prof. Dr. D. Vogt-Weisenhorn with the Golgi analyses and Dr. Stylianos Michalakis for providing us with the AAVs.

REFERENCES

Abdul HM, Sama MA, Furman JL, Mathis DM, Beckett TL, Weidner AM, Patel ES, Baig I, Murphy MP, LeVine H, 3rd, Kraner SD, Norris CM. 2009. Cognitive decline in Alzheimer's disease is associated with selective changes in calcineurin/NFAT signaling. J Neurosci 29:12957–12969.

Agarwal A, Dibaj P, Kassmann CM, Goebbels S, Nave KA, Schwab MH. 2012. In vivo imaging and noninvasive ablation of pyramidal neurons in adult NEX-CreERT2 mice. Cerebral Cortex 22:1473–1486.

Akagi K, Sandig V, Vooijs M, Van der Valk M, Giovannini M, Strauss M, Berns A. 1997. Cre-mediated somatic site-specific recombination in mice. Nucleic Acids Res 25:1766–1773.

Bartholomä A, Nave KA. 1994. NEX-1: A novel brain-specific helix-loop-helix protein with autoregulation and sustained expression in mature cortical neurons. Mech Dev 48:217–228.

Bonnerot C, Rocancourt D, Briand P, Grimber G, Nicolas JF. 1987. A beta-galactosidase hybrid protein targeted to nuclei as a marker for developmental studies. Proc Natl Acad Sci USA 84:6795–6799.

Braak H, Braak E. 1991. Neuropathological stageing of Alzheimer-related changes. Acta Neuropathol 82:239–259.

Braak H, Braak E. 2000. Pathoanatomy of Parkinson's disease. J Neurol 247:II3–II10.

Branda CS, Dymecki SM. 2004. Talking about a revolution: The impact of site-specific recombinases on genetic analyses in mice. Dev Cell 6:7–28.

Carola V, D'Olimpio F, Brunamonti E, Mangia F, Renzi P. 2002. Evaluation of the elevated plus-maze and open-field tests for the assessment of anxiety-related behaviour in inbred mice. Behav Brain Res 134:49–57.

Chishti MA, et al. 2001. Early-onset amyloid deposition and cognitive deficits in transgenic mice expressing a double mutant form of amyloid precursor protein 695. J Biol Chem 276:21562–21570.

Ciesielska A, Hadaczek P, Mittermeyer G, Zhou S, Wright JF, Bankiewicz KS, Forsayeth J. 2013. Cerebral infusion of AAV9 vector-encoding non-self proteins can elicit cell-mediated immune responses. Mol Therapy 21:158–166.

Cohen SI, Linse S, Luheshi LM, Hellstrand E, White DA, Rajah L, Otzen DE, Vendruscolo M, Dobson CM, Knowles TP. 2013. Proliferation of amyloid-beta42 aggregates occurs through a secondary nucleation mechanism. Proc Natl Acad Sci USA 110:9758–9763.

Comley LH, Wishart TM, Baxter B, Murray LM, Nimmo A, Thomson D, Parson SH, Gillingwater TH. 2011. Induction of cell stress in neurons from transgenic mice expressing yellow fluorescent protein: implications for neurodegeneration research. PloS One 6:e17639.

Crouthamel MH, Kelly EJ, Ho RJ. 2012. Development and characterization of transgenic mouse models for conditional gene knockout in the blood-brain and blood-CSF barriers. Transgenic Res 21: 113–130.

Cruz FC, Koya E, Guez-Barber DH, Bossert JM, Lupica CR, Shaham Y, Hope BT. 2013. New technologies for examining the role of neuronal ensembles in drug addiction and fear. Nat Rev Neurosci 14:743–754.

Cruz FC, Babin KR, Leao RM, Goldart EM, Bossert JM, Shaham Y, Hope BT. 2014. Role of nucleus accumbens shell neuronal ensembles in context-induced reinstatement of cocaine-seeking. J Neurosci 34:7437–7446.

Cruz FC, Javier Rubio F, Hope BT. 2015. Using c-fos to study neuronal ensembles in corticostriatal circuitry of addiction. Brain Res 1628:157–173.

Cui C, Wani MA, Wight D, Kopchick J, Stambrook PJ. 1994. Reporter genes in transgenic mice. Transgenic Res 3:182–194.

Dauer W, Przedborski S. 2003. Parkinson's disease: Mechanisms and models. Neuron 39:889–909.

de Angelis MH, et al. 2015. Analysis of mammalian gene function through broad-based phenotypic screens across a consortium of mouse clinics. Nature genetics advance online publication.

Diester I, Kaufman MT, Mogri M, Pashaie R, Goo W, Yizhar O, Ramakrishnan C, Deisseroth K, Shenoy KV. 2011. An optogenetic toolbox designed for primates. Nat Neurosci 14:387–397.

Dimri GP, Lee X, Basile G, Acosta M, Scott G, Roskelley C, Medrano EE, Linskens M, Rubelj I, Pereira-Smith O, et al. 1995. A biomarker that identifies senescent human cells in culture and in aging skin in vivo. Proc Natl Acad Sci USA 92:9363–9367.

Engeln M, Bastide MF, Toulme E, Dehay B, Bourdenx M, Doudnikoff E, Li Q, Gross CE, Boue-Grabot E, Pisani A, Bezard E, Fernagut PO. 2016. Selective inactivation of striatal FosB/Delta-FosB-expressing neurons alleviates L-dopa-induced dyskinesia. Biol Psychiatry 79:354–361.

Erdmann G, Schutz G, Berger S. 2007. Inducible gene inactivation in neurons of the adult mouse forebrain. BMC Neurosci 8:63.

Feil R, Wagner J, Metzger D, Chambon P. 1997. Regulation of Cre recombinase activity by mutated estrogen receptor ligand-binding domains. Biochem Biophys Res Commun 237:752–757.

Fujikawa Y, Kawanishi M, Kuraoka I, Yagi T. 2014. Frequencies of mutagenic translesion DNA synthesis over cisplatin-guanine intrastrand crosslinks in lacZ plasmids propagated in human cells. Mutat Res Gene Toxicol Environ Mutagenesis 770:23–28.

Gassen NC, Hartmann J, Zschocke J, Stepan J, Hafner K, Zellner A, Kirmeier T, Kollmannsberger L, Wagner KV, Dedic N, Balsevich G, Deussing JM, Kloiber S, Lucae S, Holsboer F, Eder M, Uhr M, Ising M, Schmidt MV, Rein T. 2014. Association of FKBP51 with priming of autophagy pathways and mediation of antidepressant treatment response: evidence in cells, mice, and humans. PLoS Med 11:e1001755-

Geng YQ, Guan JT, Xu XH, Fu YC. 2010. Senescence-associated beta-galactosidase activity expression in aging hippocampal neurons. Biochem Biophys Res Commun 396:866–869.

Giusti SA, Vercelli CA, Vogl AM, Kolarz AW, Pino NS, Deussing JM, Refojo D. 2014a. Behavioral phenotyping of Nestin-Cre mice: Implications for genetic mouse models of psychiatric disorders. J Psych Res 55:87–95.

Giusti SA, Vogl AM, Brockmann MM, Vercelli CA, Rein ML, Trumbach D, Wurst W, Cazalla D, Stein V, Deussing JM, Refojo D. 2014b. MicroRNA-9 controls dendritic development by targeting REST. eLife 3:

Goebbels S, Bormuth I, Bode U, Hermanson O, Schwab MH, Nave KA. 2006. Genetic targeting of principal neurons in neocortex and hippocampus of NEX-Cre mice. Genesis 44:611–621.

Golub Y, Mauch CP, Dahlhoff M, Wotjak CT. 2009. Consequences of extinction training on associative and non-associative fear in a mouse model of Posttraumatic Stress Disorder (PTSD). Behav Brain Res 205:544–549.

Grünecker B, Kaltwasser SF, Peterse Y, Sämann PG, Schmidt MV, Wotjak CT, Czisch M. 2010. Fractionated manganese injections: Effects on MRI contrast enhancement and physiological measures in C57BL/6 mice. NMR Biomed 23:913–921.

Grünecker B, Kaltwasser SF, Zappe AC, Bedenk BT, Bicker Y, Spoormaker VI, Wotjak CT, Czisch M. 2013. Regional specificity of manganese accumulation and clearance in the mouse brain: Implications for manganese-enhanced MRI. NMR Biomed 26:542–556.

Guggenhuber S, Romo-Parra H, Bindila L, Leschik J, Lomazzo E, Remmers F, Zimmermann T, Lerner R, Klugmann M, Pape H-C, Lutz B. 2016. Impaired 2-AG signaling in hippocampal glutamatergic neurons: Aggravation of anxiety-like behavior and unaltered seizure susceptibility. Int J Neuropsychopharmacol 19:pyv091.

Hardy J, Selkoe DJ. 2002. The amyloid hypothesis of Alzheimer's disease: Progress and problems on the road to therapeutics. Science (New York, NY) 297:353–356.

Hoess RH, Ziese M, Sternberg N. 1982. P1 site-specific recombination: nucleotide sequence of the recombining sites. Proc Natl Acad Sci USA 79:3398–3402.

Jacob W, Yassouridis A, Marsicano G, Monory K, Lutz B, Wotjak CT. 2009. Endocannabinoids render exploratory behaviour largely independent of the test aversiveness: Role of glutamatergic transmission. Genes Brain Behav 8:685–698.

Jinno S, Kosaka T. 2010. Stereological estimation of numerical densities of glutamatergic principal neurons in the mouse hippocampus. Hippocampus 20:829–840.

Kamprath K, Wotjak CT. 2004. Nonassociative learning processes determine expression and extinction of conditioned fear in mice. Learn Memory 11:770–786.

Kassem MS, Lagopoulos J, Stait-Gardner T, Price WS, Chohan TW, Arnold JC, Hatton SN, Bennett MR. 2013. Stress-induced grey matter loss determined by MRI is primarily due to loss of dendrites and their synapses. Mol Neurobiol 47:645–661.

Kleinknecht KR, Bedenk BT, Kaltwasser SF, Grunecker B, Yen YC, Czisch M, Wotjak CT. 2012. Hippocampus-dependent place learning enables spatial flexibility in C57BL6/N mice. Front Behav Neurosci 6:87.

Kobayashi DT, Chen KS. 2005. Behavioral phenotypes of amyloid-based genetically modified mouse models of Alzheimer's disease. Genes Brain Behav 4:173–196.

Koya E, Golden SA, Harvey BK, Guez-Barber DH, Berkow A, Simmons DE, Bossert JM, Nair SG, Uejima JL, Marin MT, Mitchell TB, Farquhar D, Ghosh SC, Mattson BJ, Hope BT. 2009. Targeted disruption of cocaine-activated nucleus accumbens neurons prevents context-specific sensitization. Nat Neurosci 12:1069–1073.

Li P, Tong C, Mehrian-Shai R, Jia L, Wu N, Yan Y, Maxson RE, Schulze EN, Song H, Hsieh C-L, Pera MF, Ying Q-L. 2008. Germline competent embryonic stem cells derived from rat blastocysts. Cell 135:1299–1310.

Lu A, Steiner MA, Whittle N, Vogl AM, Walser SM, Ableitner M, Refojo D, Ekker M, Rubenstein JL, Stalla GK, Singewald N, Holsboer F, Wotjak CT, Wurst W, Deussing JM. 2008. Conditional mouse mutants highlight mechanisms of corticotropin-releasing hormone effects on stress-coping behavior. Mol Psychiatry 13:1028–1042.

Madisen L, et al. 2012. A toolbox of Cre-dependent optogenetic transgenic mice for light-induced activation and silencing. Nat Neurosci 15:793–802.

Monory K, et al. 2006. The endocannabinoid system controls key epileptogenic circuits in the hippocampus. Neuron 51:455–466.

Mota E, Sousa F, Sousa A, Queiroz JA, Cruz C. 2014. Molecular recognition of oligonucleotides and plasmid DNA by l-methionine. J Mol Recogn 27:588–596.

Nakamura T, Colbert MC, Robbins J. 2006. Neural crest cells retain multipotential characteristics in the developing valves and label the cardiac conduction system. Circulation Res 98:1547–1554.

Nolan GP, Fiering S, Nicolas JF, Herzenberg LA. 1988. Fluorescence-activated cell analysis and sorting of viable mammalian cells based on beta-D-galactosidase activity after transduction of Escherichia coli lacZ. Proc Natl Acad Sci USA 85:2603–2607.

Perisic T, Zimmermann N, Kirmeier T, Asmus M, Tuorto F, Uhr M, Holsboer F, Rein T, Zschocke J. 2010. Valproate and amitriptyline exert common and divergent influences on global and gene promoter-specific chromatin modifications in rat primary astrocytes. Neuropsychopharmacology 35:792–805.

Plendl W, Wotjak CT. 2010. Dissociation of within- and between-session extinction of conditioned fear. J Neurosci 30:4990–4998.

Preibisch S, Saalfeld S, Tomancak P. 2009. Globally optimal stitching of tiled 3D microscopic image acquisitions. Bioinformatics 25: 1463–1465.

Price J, Turner D, Cepko C. 1987. Lineage analysis in the vertebrate nervous system by retrovirus-mediated gene transfer. Proc Natl Acad Sci USA 84:156–160.

Refojo D, Schweizer M, Kuehne C, Ehrenberg S, Thoeringer C, Vogl AM, Dedic N, Schumacher M, von Wolff G, Avrabos C, Touma C, Engblom D, Schutz G, Nave KA, Eder M, Wotjak CT, Sillaber I, Holsboer F, Wurst W, Deussing JM. 2011. Glutamatergic and dopaminergic neurons mediate anxiogenic and anxiolytic effects of CRHR1. Science (New York, NY) 333:1903–1907.

Reichel JM, Nissel S, Rogel-Salazar G, Mederer A, Käfer K, Bedenk BT, Martens H, Anders R, Grosche J, Michalski D, Härtig W, Wotjak CT. 2015. Distinct behavioral consequences of short-term and prolonged GABAergic depletion in prefrontal cortex and dorsal hippocampus. Front Behav Neurosci 8.

Ross CA, Tabrizi SJ. 2011. Huntington's disease: From molecular pathogenesis to clinical treatment. Lancet Neurol 10:83–98.

Sanes JR, Rubenstein JL, Nicolas JF. 1986. Use of a recombinant retrovirus to study post-implantation cell lineage in mouse embryos. EMBO J 5:3133–3142.

Schmidt-Supprian M, Rajewsky K. 2007. Vagaries of conditional gene targeting. Nat Immunol 8:665–668.

Schmidt A, Tief K, Foletti A, Hunziker A, Penna D, Hummler E, Beermann F. 1998. lacZ transgenic mice to monitor gene expression in embryo and adult. Brain Res Brain Res Protocols 3:54–60.

Schönig K, Weber T, Frommig A, Wendler L, Pesold B, Djandji D, Bujard H, Bartsch D. 2012. Conditional gene expression systems in the transgenic rat brain. BMC Biol 10:77.

Schumann Burkard G, Jutzi P, Roditi I. 2011. Genome-wide RNAi screens in bloodstream form trypanosomes identify drug transporters. Mol Biochem Parasitol 175:91–94.

Schwab MH, Druffel-Augustin S, Gass P, Jung M, Klugmann M, Bartholomae A, Rossner MJ, Nave KA. 1998. Neuronal basic helix-loop-helix proteins (NEX, neuroD, NDRF): Spatiotemporal expression and targeted disruption of the NEX gene in transgenic mice. J Neurosci 18:1408–1418.

Skarnes WC, Rosen B, West AP, Koutsourakis M, Bushell W, Iyer V, Mujica AO, Thomas M, Harrow J, Cox T, Jackson D, Severin J, Biggs P, Fu J, Nefedov M, de Jong PJ, Stewart AF, Bradley A. 2011. A conditional knockout resource for the genome-wide study of mouse gene function. Nature 474:337–342.

Soriano P. 1999. Generalized lacZ expression with the ROSA26 Cre reporter strain. Nat Gene 21:70–71.

Stühmer T, Puelles L, Ekker M, Rubenstein JL. 2002. Expression from a Dlx gene enhancer marks adult mouse cortical GABAergic neurons. Cerebral Cortex 12:75–85.

Sweatt JD. 2004. Hippocampal function in cognition. Psychopharmacology 174:99–110.

Tong C, Li P, Wu NL, Yan Y, Ying Q-L. 2010. Production of p53 gene knockout rats by homologous recombination in embryonic stem cells. Nature 467:211–213.

Vyas A, Mitra R, Shankaranarayana Rao BS, Chattarji S. 2002. Chronic stress induces contrasting patterns of dendritic remodeling in hippocampal and amygdaloid neurons. J Neurosci 22: 6810–6818.

Weiss DJ, Liggitt D, Clark JG. 1997. In situ histochemical detection of beta-galactosidase activity in lung: assessment of X-Gal reagent in distinguishing lacZ gene expression and endogenous beta-galactosidase activity. Human Gene Therapy 8:1545–1554.

White JK, et al. 2013. Genome-wide generation and systematic phenotyping of knockout mice reveals new roles for many genes. Cell 154:452–464.

Witten IB, Steinberg EE, Lee SY, Davidson TJ, Zalocusky KA, Brodsky M, Yizhar O, Cho SL, Gong S, Ramakrishnan C, Stuber GD, Tye KM, Janak PH, Deisseroth K. 2011. Recombinase-driver rat lines: tools, techniques, and optogenetic application to dopamine-mediated reinforcement. Neuron 72:721–733.

Yen YC, Anderzhanova E, Bunck M, Schuller J, Landgraf R, Wotjak CT. 2013. Co-segregation of hyperactivity, active coping styles, and cognitive dysfunction in mice selectively bred for low levels of anxiety. Front Behav Neurosci 7:103-

Zschocke J, Zimmermann N, Berning B, Ganal V, Holsboer F, Rein T. 2011. Antidepressant drugs diversely affect autophagy pathways in astrocytes and neurons–dissociation from cholesterol homeostasis. Neuropsychopharmacology 36:1754–1768.